REVIEW

Recent Advances in Exploring Highly Active & Durable PGM-Free Oxygen Reduction Catalysts

Yuan Li, Miao-Ying Chen, Bang-An Lu*, Jia-Nan Zhang*

College of Materials Science and Engineering, Zhengzhou University, Zhengzhou 450001, PR China

Abstract

In order to reduce the considerable usage of expensive but scarce platinum at the cathode in proton exchange membrane fuel cells (PEMFCs), it is necessary to pursue alternatives to platinum. The most promising platinum group metal (PGM)-free catalysts for oxygen reduction reaction (ORR) are atomically dispersed, and nitrogen-coordinated metal site catalysts denoted as M-N-C (M = Fe, Co, or Mn, etc.). Over the last few decades, there have been great advances in these catalysts with high ORR activity and promising initial fuel cell performance approaching traditional Pt/C catalysts. However, the stability of these highly active Fe-N-C catalysts under practical fuel cell conditions is still far from satisfactory. This review highlights recent advances in synthesizing efficient PGM-free catalysts for the ORR in PEMFCs, emphasizing our efforts on confinement strategies and spin state regulation methods. We also summarize several effective methods of improving mass and intrinsic activities. Furthermore, significant research efforts toward understanding the degradation mechanisms are made and the results are summarized, such as metal leaching, carbon corrosion, protonation, and micropore flooding. We also document several mitigation strategies to improve the lifetime of PGM-free catalysts, including controlling S1/S2 in Fe-N-C catalysts, using non-iron-based catalysts, enhancing metal-nitrogen bonds, improving the corrosion resistance of carbon carriers, and using buffered protonated liquids. Finally, the remaining challenges and possible solutions to the current atomic dispersion M-N-C catalyst are proposed in detail.

Keywords: PGM-free catalyst; Confinement strategy; Spin state regulation; Degradation mechanism; Mitigation strategy

1. Introduction

The burning of fossil fuels produces the vast majority (>85 percent) of the energy used in stationary and automotive applications worldwide. When fossil fuels are consumed in internal-combustion engines, however, a considerable number of pollutants, including NO_x, SO_x, and particulates, are created, which are damaging to the environment. Clean electric vehicles can be powered by proton exchange membrane fuel cells (PEMFCs), which transform hydrogen's chemical energy into electricity [1]. The slow kinetics of the cathodic oxygen reduction (ORR) process, which requires significant amounts of expensive and scarce platinum, obstructs large-scale use of PEMFCs, necessitating Pt-group-metal-free (PGM-free) catalysts as low-cost alternatives [2].

There have been significant developments in the mechanistic understanding of ORR, new catalyst synthesis methods, and overall performance improvements during the previous few decades [3−13]. Due to their intrinsically high ORR activity and reasonable stability under the relevant acidic environments desirable for PEMFCs, metal-nitrogen-carbon catalysts (M-N-C, M = Fe, Co, Mn, etc.) have emerged as the most promising PGM-free catalysts [4,7,12,14]. Among all M-N-C catalysts, Fe-N-C has attracted the most attention because of its highest activity in acidic media. The past decade has witnessed rapid progress in Fe-N-C activity, especially confinement methods based on the zeolitic imidazolate framework [6,13], representing the key to developing efficient Fe-N-C catalysts containing atomically dispersed and nitrogen-coordinated single metal active sites (i.e.,

Received 30 May 2022; Revised 13 June 2022; Accepted 21 June 2022; Available online 5 July 2022

* Corresponding author, Bang-An Lu, Tel: (86-371)67781590, E-mail address: balu@zzu.edu.cn.
* Corresponding author, Jia-Nan Zhang, Tel: (86-371)67781590, E-mail address: zjn@zzu.edu.cn.

https://doi.org/10.13208/j.electrochem.2215002

MN_4). For example, the latest Fe-N-C catalyst reported by Wu's group shows a recorded high half-wave potential of 0.915 V (vs. RHE) in 0.5 $mol \cdot L^{-1}$ H_2SO_4. Fe-N-C cathodes with a loading of 4 $mg \cdot cm^{-2}$ in MEAs also demonstrated performance approaching that of a typical Pt/C cathode (0.1 $mg_{Pt} \cdot cm^{-2}$), especially in kinetic ranges [15]. Challenging activity targets have been set for PGM-free catalysts by the US Department of Energy (DOE); for example, a current density of 0.044 $A \cdot cm^{-2}$ under 1.0 bar H_2-O_2 at 0.9 $V_{iR\text{-}free}$ as the 2020 target.

While the activity is encouraging, the stability of these highly active Fe-N-C catalysts under practical fuel cell conditions is still far from satisfactory [4,5,16−19]. The stability of Fe-N-C is usually measured by chronoamperometry at the cell voltage of 0.4−0.7 V. A performance loss of 40%-80% typically occurs during the first 100 h of fuel cell testing at the cell voltage of 0.4−0.7 V, hardly meeting the durability target of 8000 h drive cycle with startup/shutdown or equivalent accelerated stress test procedures [20].

We first highlight recent advancements in this review, with an emphasis on our attempts to construct viable PGM-free catalysts using spatial confinement and chemical binding atomic confinement. To demonstrate the effectiveness of the related confinement strategies, we illustrate the representative examples. Then we focus on the effects of spin state management on activity, and additional common beneficial strategies emerged. Afterwards, we go over the various degradation mechanisms that have emerged in recent decades and the current state of knowledge about how the fine structures of the active site affect the durability, such as metal leaching, carbon corrosion, protonation, and micropore flooding. We also detail potential mitigating measures for extending the lifetime of PGM-free catalysts, such as employing non-iron-based catalysts, increasing metal-nitrogen bonding, and improving catalyst performance. Finally, the remaining challenges and perspectives are proposed for the precise construction of next-generation M-N-C electrocatalysts via integrated strategies at multiscale to meet the requirements of practical fuel cells.

2. Activity regulation of non-noble metal oxygen reduction catalysts for proton exchange membrane fuel cells

Metal atoms frequently aggregate spontaneously during the production of conventional M-N-C catalysts since M−M bonds are more thermodynamically stable than M−N bonds. These metal nanoparticles diminish the density of M−N bonds and eliminate the catalyst's source of active sites. As a result, we must limit the spontaneous aggregation of metal atoms and convert the metal atoms in the precursors directly into the active groups of M−N atoms. Briefly, the catalyst activity can be regulated in two ways [10−12,21−30]: (1) to improve the intrinsic catalyst activity by changing the electron distribution in the active center of the catalyst, thus improving the adsorption behavior to the ORR reaction intermediates; (2) to increase the site density of the catalyst. Since previous remarkable reviews have summarized many effective methods to enhance the activity of PGM-free catalysts, herein we mainly focus on our efforts in spatial confinement, chemical binding atomic confinement and spin state regulation of metal center. In the final of this part, we will briefly introduce several typical methods developed by other groups.

2.1. Spatial confinements

Tremendous efforts have shown that controlling the structural features of catalysts can improve their performance toward ORR [13,31−33]. To this end, various confinement strategies have been proposed to precisely control the dimensions of catalysts during their formation. The limited spaces used in the confinement synthesis not only act as a physical reactor to define the shape and size of products, but also enable the precise synthesis of uniform and nanosized metal clusters as electrocatalysts while preventing them from aggregation. In 2013, Bao's group encapsulated Fe nanoparticles (NPs) into the compartments of peapod like carbon nanotubes (CNTs) through one-step synthesis at 350 °C in N_2 using ferrocene and sodium azide as the precursors [34]. In this type of spatial confinement catalyst, the stable carbon layer can protect the inner metal from the damaging effects of the reaction environment, and electron transfer from the active metal core to the carbon layer excites the unique catalytic activity on the carbon surface. The catalytic activity depends on how much the surface is activated by the encapsulated inner NPs and also how much the surface is enriched with electrons coming from the inner NPs, which is strongly related to the thickness of the chain-mail layer. The surface of an over-thick chain-mail layer is barely affected by the inner NPs. Recently, they clarified the thickness effect of a graphene-like carbon layer and showed that the electrons of the inner NPs can traverse up to three carbon layers before the effect becomes too weak (Fig. 1A) [34]. Thus, the chain-mail surface is not likely to be activated if the layer

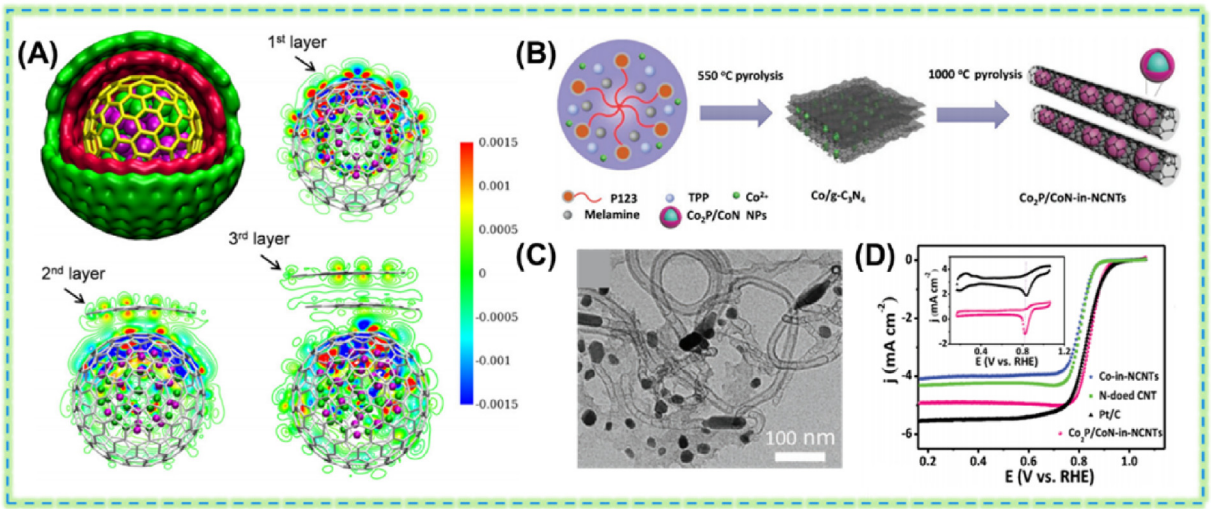

Fig. 1. (A) Differential charge density of chain mail catalyst, CoNi alloy nanoparticles are encapsulated in two and three carbon layers. Reproduced with permission of Ref. [34] Copyright 2020, John wiley. (B) The synthetic route for Co_2P/CoN-in-NCNTs. Reproduced with permission of Ref. [24] Copyright 2018, John wiley. (C) TEM image of Co_2P/CoN-in-NCNTs. (D) LSV curves of Co_2P/CoN-in-NCNTs, Co-in-NCNTs, N-doped CNT, and Pt/C catalysts in O_2-saturated 0.1 mol·L^{-1} KOH solution. (color on line).

number is greater than three. Tuning the atomic composition of the chain-mail layer by doping with heteroatoms can influence the charge redistribution as well as the activity of the chain-mail surface.

Our group also has made tremendous contributions to spatial confinement catalysts [10,11,21,24,26,27]. In 2018, we developed a facile one-step self-assembly and confined pyrolysis approach to obtain Co_2P-CoN core-shell NPs encapsulated in N-doped carbon nanotubes (Co_2P/CoN-in-NCNTs). Benefiting from the synergistic effects between Co_2P/CoN NPs double active sites and porous conductive N-doped carbon networks, the Co_2P/CoN-in-NCNTs catalyst delivered superior ORR activity with a half-wave potential ($E_{1/2}$) of 0.85 V versus RHE and high durability (almost no decay after 5000 cycles) [24]. Afterward, our group synthesized an atomically dispersed FeNC-S-Fe_xC/Fe catalyst through the pyrolysis of microporous carbon fibers coated with zeolite imidazolate framework (ZIF), sulfurization and pyrolysis synthesis simultaneously [25]. During pyrolysis, Zn atoms are evaporated, leaving Fe, N, and S embedded in the carbon structure, and high-resolution TEM images show a one-dimensional carbon nanotube (CNF_s) formed by ZIF-8-derived "carbon boxes" adhering to carbon nanofibers, forming hierarchical micropores that can facilitate material transport and in accelerating electrochemical reaction kinetics. The half-wave potential of FeNC-S-Fe_xC/Fe catalyst was 0.821 V, 180 mV higher than that of FeNC-Fe_xC/Fe, and even better than Pt/C. Based on HAADF-STEM, XANES, and EXAFS analyses, we found that the Fe—S bonds formed at the interface between the Fe_xC/Fe clusters and S-containing Fe-N-C matrix result in new types of active sites that can increase the activity of bifunctional catalysts for oxygen reactions. DFT calculations further confirmed that the atomically dispersed FeN_x sites of the Fe-N-C system, the Fe_xC clusters, and the S-containing sites are the active species and that their interactions play a significant role in catalytic activity.

As mentioned above, the activity and stability of spatial confinements catalysts depend on the thickness of carbon layer. In the context of activity, the carbon layer number should be less than three. However, the stability may suffer severe damage in harsh environments if the chain-mail layer is too thin and it may also bring the risk of low catalytic durability in harsh reaction environments. As such, how to optimize the thickness of carbon layers is essential to balance of the catalytic activity and durability. Furthermore, the encapsulated metal NPs are the origin of the reactivity and the source of the redistributed electrons. Thus, their metallicity accounts for the efficacy of enhancing the activity of the outermost carbon layer.

2.2. Chemical confinements

Because M—M bonds are more thermodynamically stable than M—N bonds, metal atoms frequently aggregate spontaneously during the production of conventional M-N-C catalysts. As such, considerable efforts have been invested in the past few decades to seek effective precursors and optimal support/templates to increase site density. The design of suitable chemical binding

between the active metal center and the substrate can restrain the metal atom during the synthesis of SACs, making it possible for metal centers to disperse on the substrate at the atomic level [3,23,24,29]. The defects will change the coordination of the surrounding electronic structure. These defects on the substrate can capture metal precursors and anchor metal atoms for post-processing. By capturing metal atoms through the defect carbon, the catalyst with high activity can be designed reasonably. Recently, our group synthesized Fe-N-C-P/N,P-C through the driving strategy of phosphorus doping affecting the electronic structure of the marginal FeN_4 active site (Fig. 2A) [29]. Fe-N-C-P/N,P-C shows an intense peak at 1.50 Å in the FT-EXAFS spectrum, with no significant peaks corresponding to Fe-Fe coordination at 2.20 and 4.42 Å (Fig. 2B). In contrast to FePc, where a shell of four N atoms surrounds a Fe atom, it was experimentally demonstrated that the Fe-N-C-P/N,P-C sample has more edge-type FeN_4 molecules and that the addition of P inhibits the formation of Fe particles; thus, contributing to stabilize the active site in Fe-N-C. As shown in Fig. 2C, Fe-N-C-P/N,P-C showed the best electrocatalytic performance with $E_{1/2}$ of 0.80 V in O_2-saturated 0.1 mol·L^{-1} $HClO_4$ at 1600 rpm. These results indicate that doping P at the active site of FeN_4 at the edge of carbon nanocages does improve the activity of ORR. Then, our group put forward Co-N-C active sites confined in N, B-co-doped carbon nanosheets (Co-N,B-CSs) via the self-assembly pyrolysis method using a soft template (Fig. 2D) [23]. The EXAFS analysis clearly shows that no Co-Co interaction is observed in the Co-N,B-CSs and no Co-O peak in 1.64 Å. This also confirms that these two samples are not cobalt oxide. This indicates that Co is well-distributed atom in the carbon network (Fig. 2E). The performance of Co-N, B-CSs in O_2-saturated 0.1 mol·L^{-1} KOH is comparable to that of commercial Pt/C with an $E_{1/2}$ of 0.83 V (Fig. 2F). The introduction of B atoms facilitates the capture of oxygen species, thus accelerating the ORR four-electron process. In this regard, the local coordination structure of the metal center can be adjusted by changing the number of coordinated N ligands and doping additional heteroatoms (e.g., B, S, or P) into the carbon planes. The kinetic activity of active sites can be governed by their surrounding carbon structures, thereby improving the ORR activity. A deep understanding of the correlation between the active site affected by the dopant atoms and the catalytic performance is of great interest in the future.

2.3. Spin state regulation strategies

In addition to increasing active site density for improving mass activity, it is essential to enhance the intrinsic activity of M-N-C active sites for superseding catalyst performance. For stable atom-classified M-N-C catalysts, adjusting the spin state of the active center atom, the adsorption energy of

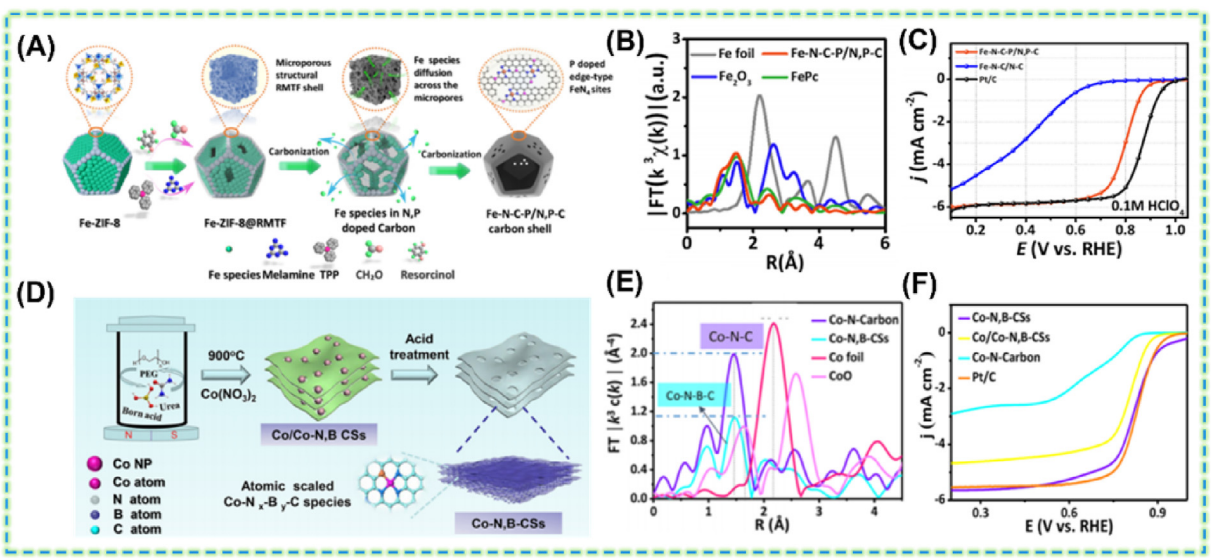

Fig. 2. (A) Synthesis and TEM characterizations of Fe-N-C-P/N,P-C. Reproduced with permission of Ref. [29] Copyright 2021, American Chemical Society. (B) Fourier transformed EXAFS spectra of Fe-N-C-P/N,P-C and reference materials. (C) LSV curves of ORR in O_2-saturated 0.1 mol·L^{-1} $HClO_4$ at 1600 rpm for Fe-N-C-P/N,P-C, and reference materials. (D) Synthetic procedure of the Co/N-B-doped carbon nanosheet (Co-N,B-CSs). Reproduced with permission of Ref. [23] Copyright 2018, American Chemical Society (E) Fourier transformed EXAFS spectra of the Co-N,B-CSs and reference materials. (F) LSV curves of Co/Co-N,B-CSs and reference materials in O_2-saturated 0.1 mol·L^{-1} KOH solution. (color on line).

the ORR intermediate can be improved effectively, and the activity of the catalyst can be increased. In 2019, our group synthesized FePc@N,P-DC catalyst by coordinating a non-pyrolytic strategy of M-N_4 organic macro-ring molecules anchored on N-doped defective carbon nanosheets (Fig. 3A) [21]. Through magnetic susceptibility measurement and electron paramagnetic resonance spectrum, the electron spin configuration of FeN_4 part of FePc molecule was revealed. Unpaired electrons gaining or losing angular momentum can change the value of its G factor, FePc@N,P-DC showed slight changes. This suggests that topological defects contribute to changing the 3d spin configuration and chemical environment. Medium-spin and high-spin Fe having different $dxy^2dyz^2dxz^1dz2^1$ and $dxy^2dyz^1dxz^1dz2^1dxy^1$ (Fig. 3B) defective carbons promote the high-spin state of the Fe center in FePc molecules. In O_2-saturated 0.1 mol·L^{-1} $HClO_4$ solution FePc@N, P-DC had the highest ORR catalytic activity with $E_{1/2}$ of 0.903 V (Fig. 3C). P doping sites play an important role in regulating the charge distribution of the carbon skeleton and even the active center of Fe-N_4, thus optimizing the adsorption behavior and adjusting the activity of the electrochemical catalyst.

Recently, Our group introduced Mn-N bonds into traditional Fe/N-C systems by pre-polymerization and pyrolysis (Fig. 3D) [35]. The introduction of the Mn-N part leads to the delocalization of the Fe^{III} electron, which makes the spin state of Fe^{III} transition from low-spin ($t_{2g}5e_g0$) to medium-spin ($t_{2g}4e_g1$), and easily penetrates the antibonding π-orbital of oxygen, resulting in good ORR activity [28]. To elucidate the electron spin configurations of Fe, Mn/N-C, we calculate the effective magnetic moments Fe,Mn/N-C, and Fe/N-C of 3.75 μ_{eff} and 2.16 $\mu_{eff,}$ respectively, by measuring the temperature-dependent susceptibility of zero-field cooling (ZFC) (Fig. 3e and F). In addition, we further obtained the number of unpaired d electrons (n) of Fe^{III} ion by the following formula:

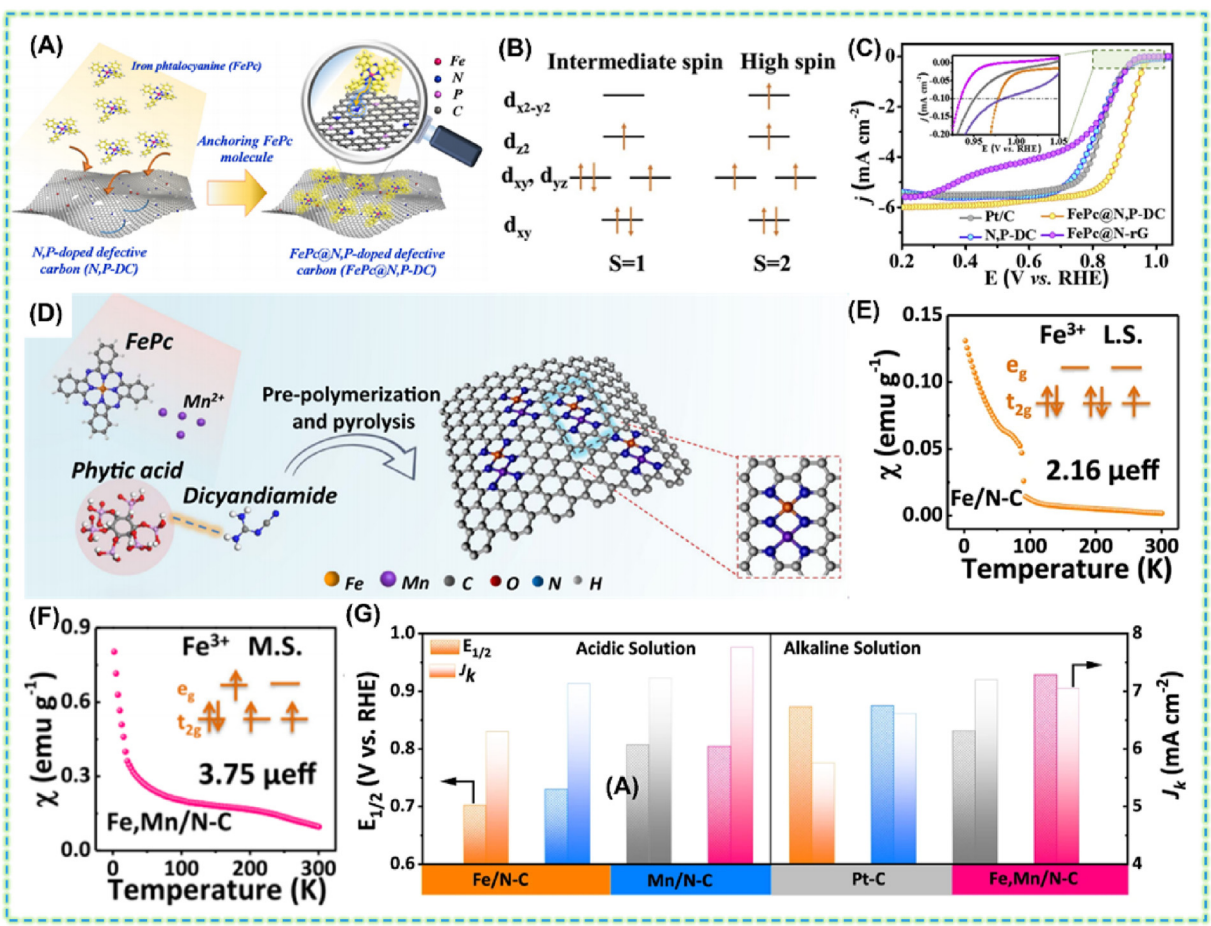

Fig. 3. (A) Synthetic procedure of FePc@N,P-DC catalyst. Reproduced with permission of Ref. [21] Copyright 2020, Elsevier. (B) Schematic representation of the spin transition of Fe. (C) LSV curves of ORR in O_2-saturated 0.1 mol·L^{-1} KOH at 1600 rpm for different catalysts. Inset is amplifying picture at onset potential, (D) Schematic illustration of synthesis procedure for Fe,Mn/N-C catalysts. Reproduced with permission of Ref. [35] Copyright 2021, Nature groups. (E) Fe/N-C, (F) Fe,Mn/N-C (M.S. represents medium-spin, and L.S. represents low-spin), (G) Comparison of the kinetic current density (J_k) and $E_{1/2}$ of Fe,Mn/N-C, Fe/N-C, Mn/N-C, and Pt/C catalysts. (color on line).

$$\mu_{eff} = \sqrt{n(n+2)} \quad (1)$$

The unpaired d electron (n) number of Fe/N-C is about 1.3, which means that the Fe^{III} ion has a low-spin state and is not filled, so there is no electron occupied in the σ* antibonding orbital of FeN_4, resulting in a very strong Fe^{III}/O_2 interaction and a fairly stable $Fe^{4+}-O_2^{2-}$ bond. Fe has about three unpaired d electrons, and it has been single e_g filling. Through LSV tests, the $E_{1/2}$ of Fe,Mn/N-C in 0.1 mol·L^{-1} $HClO_4$ solution was 0.804 V, while 0.928 V in 0.1 mol·L^{-1} KOH solution, comparable to that of commercial Pt/C (Fig. 3G). The distribution of 3d orbital electrons in metal centers of transition elements will affect the chemical environment of active centers. Even with the same valence, different spin states exhibit different oxygen reduction activities. It can be adjusted by doping heteroatoms and introducing metal atoms.

2.4. Other effective methods

Besides the above methods, there are also tremendous and effective methods developed by other groups, which have been summarized by many remarkable reviews [4,8,35]. Herein, we briefly introduce some typical methods as follows.

Due to the thick catalysts layer, the mesoporous structure of M-N-C is key to the performance of fuel cells. By heating the outer surface of ZIF-8 with SiO_2-coated argon at 650 °C, the concave SiO_2@Z8-650 was synthesized by shui and collaborators [5]. The silicon layer was then etched, and iron atoms were introduced to form TPI@Z8(SiO_2)-650-C with a mesoporous structure (Fig. 4A). Three representative catalysts were measured at 2.5 bar H_2-O_2. TPI@Z8(SiO_2)-650-C exhibited outstanding kinetic activity with a current density of 560 mA·cm^{-2} at 0.8 V. However, TPI@Z8-650-C showed a rapid drop in voltage, reflecting the poor material transport capacity of traditional microporous solid NPs. Because the peak power density (P_{max}) was controlled by both mass transfer and kinetics, TPI@Z8(SiO_2)-650-C had a P_{max} of 1.18 W·cm^{-2} at 0.47 V, compared to a lower P_{max} of 0.85 W·cm^{-2} with TPI@Z8-650-C (Fig. 4B). This indicates that the larger surface area and mesoporous structure are favorable for the exposed FeN_4 site and the enhanced material transport of the catalytic layer. The performance of the catalyst was

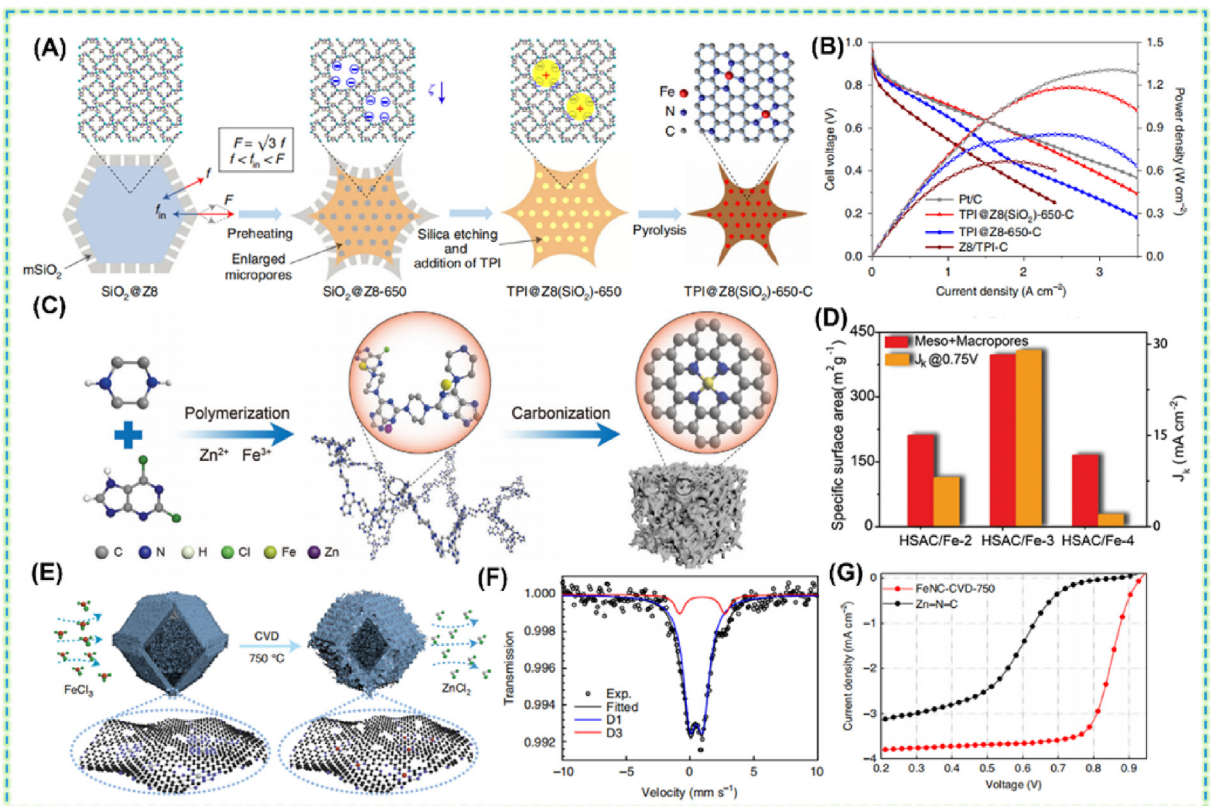

Fig. 4. (A) A schematic synthesis process of TPI@Z8(SiO_2)-650-C. Reproduced with permission of Ref. [5] Copyright 2019, Springer Nature. (B) Polarization and power density curves of the indicated catalysts. (C) A schematic synthesis process of HSAC/Fe-X catalyst. Reproduced with permission of Ref. [18] Copyright 2021, John Wiley. (D) The sum specific surface area of mesopores and macropores, J_k at 0.75 V. (E) Schematic of the high-temperature trans-metalation. Reproduced with permission of Ref. [4] Copyright 2021, Springer Nature. (F) ^{57}Fe Mössbauer spectrum at 5 K of FeNC-CVD-750. (G) Steady-state RDE polarization curves in O_2-saturated 0.5 mol·L^{-1} H_2SO_4 at room temperature, 900 rpm.

optimized by adjusting the amount of metal doping.

Xiang and co-workers synthesized Fe-N_X oxygen reduction catalysts on atomically dispersed layered porous carbon nanostructures by pre-designing layered covalent organic polymers (COP) to anchor iron (Fig. 4C) [18]. The COP materials formed a large number of microporous and mesoporous structures during sintering, which facilitated the exposure of active sites, improved the effective utilization of active sites, and promoted material transport. The HSAC/Fe-3 catalyst had a much higher kinetic current density (J_k) at 0.75 V than HSAC/Fe-2 and HSAC/Fe-4 catalysts. These results indicate that the porosity of the catalyst plays an essential role in the activity of the ORR catalyst (Fig. 4D). The mesoporous COP material helps to prepare efficient single-atom catalysts for PEMFC applications.

Li et al. prepared Fe-N-C electrocatalysts with higher active site density by using chemical vapor deposition method (Fig. 4E), and they synthesized Fe-N-C by flowing ferric chloride vapor on Zn-N-C supports at 750 °C, thereby high-temperature trans-metallization shift of Zn-N_4 sites into Fe-N_4 sites [4]. Various characterization methods show that the Fe-N-C prepared by this method has about 90% Fe-N_4 sites, all of which are gas-phase accessible active Fe sites (D1 species in Fig. 4F attributed to the Fe-N_4 site). The oxygen reduction reaction performance of Fe-N-C electrocatalyst was tested using the rotating disk electrode, and Fe-N-C ($E_{1/2}$ = 0.85 V) was found to have superior ORR activity far exceeding Zn-N-C in 0.5 mol·L^{-1} H_2SO_4 electrolyte. The controllable preparation of highly accessible Fe sites has become an effective way to enhance ORR activity.

All in all, the activity of the catalyst is improved mainly in two aspects: either the electron distribution of the active center is changed or the intrinsic activity of catalyst is changed, so as to change the adsorption behavior of ORR reaction intermediates and improve the ORR activity. Through restriction strategy, heteroatom doping, pore structure design and other means to increase the active sites of the catalyst, or improve the intrinsic activity, or both.

3. Degradation mechanisms

Among the developed PGM-free catalysts, metal-nitrogen-carbon catalysts (M-N-C, M = Fe, Co, Mn, etc.) are the most promising catalysts for fuel cells [7,17,36,37]. Their initial fuel cell performance can currently be close to that of a Pt-based cathode under low load. However, the stability of these highly active PGM-free catalysts under actual fuel cell conditions is far from satisfactory [1,38]. When M-N-C catalysts were applied to fuel cells, two stages of catalyst decay trends were observed by chronopotentiometry methods, divided into early rapid decay and late slow decay [39]. The stability target for M-N-C catalyst is less than 10% decay in 1000 h, but the existing catalysts are unstable, decaying up to 80% in 50 h. In order to commercialize a PGM-free catalyst, limited stability must be achieved [40]. Therefore, it is of great significance to study the degradation mechanism of catalysts and put forward mitigation strategies. A sea of experimental studies have shown that the overall performance of the catalyst depends on the density of the active site (SD), the intrinsic activity (TOF) of the individual site, and the accessibility of the reactants [4,6,41]. In this context, four main degradation mechanisms of PGM-free catalysts have been proposed including (i) demetallation, (ii) carbon oxidation, (iii) protonation, and (iv) microporous watering (Fig. 5A) [42].

3.1. Demetallation

For non-precious metal catalysts, the high activity sites must involve metals, and a large amount of experimental data confirms the important role of MN_x molecules, and metal clusters without graphite protection cannot exist stably in fuel cells [43,44]. The metal leaching from PGM-free catalysts has been investigated for a long time. The main challenge lies in the complex heterostructure of the catalyst and the lack of operando characterization methods [45,46]. Therefore, it is difficult to identify the metal moieties that are easily leached out and whether they are responsible for performance degradation. Furthermore, the catalyst transition metal leaching reduces the fuel cell performance and attacks the proton membrane, and reduces the ionic conductivity [14, 45, 47].

The leaching of metals in catalyst degradation is closely related to the metal species [39]. Wu et al. immobilized the ligand-chelated CoN_x moiety in the micropores of ZIF-8 through a solution synthesis route to form atomically dispersed Co, and prepared Fe-N-C catalysts by the same method [36]. Using Fe-N-C and Co-N-C for durability test, Co-N-C MEA retained 50% of its initial current density after 50 h test, while Fe-N-C MEA retained <5% (Fig. 5B). The difference in the stabilities of Fe-N-C and Co-N-C may be related to the fact that the active site in Fe-N-C is more likely to participate in or promote the Fenton reaction, resulting in the loss of the active site. Electrochemical cycling of these two catalysts in 0.5 mol·L^{-1} H_2SO_4 saturated with Ar and O_2 from 0.6 to 1.0 V (vs. RHE)

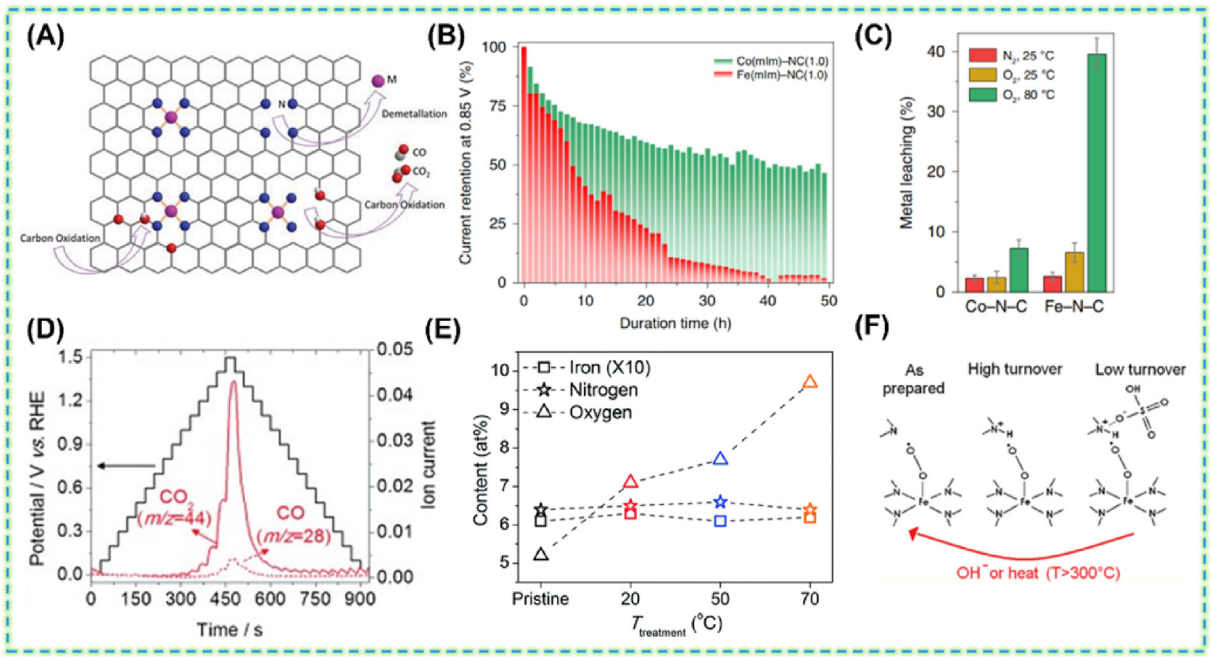

Fig. 5. ***(A)*** *Main reasons for the instability of PGM-free catalysts for the ORR in an acidic medium. Reproduced with permission of Ref. [48] Copyright 2022, American Chemical Society.* ***(B)*** *Normalized current density at a voltage of 0.85 V after voltage-step cycling (0.4 V for 55 min and 0.85 V for 5 min) for 50 h. Reproduced with permission of Ref. [36] Copyright 2020, Springer Nature.* ***(C)*** *ICP-OES results of the metal leaching experiments.* ***(D)*** *Online SFC/DEMS results. The DEMS signals were collected during a stepwise chronoamperometric experiment between 0 and 1.5 V at 50 °C. All the experiments were performed in a de-aerated 0.1 mol·L^{-1} $HClO_4$ electrolyte. Reproduced with permission of Ref. [19] Copyright 2015, John Wiley.* ***(E)*** *Measurements of N and O by XPS and Fe by ICP. Reproduced with permission of Ref. [49] Copyright 2018, Royal Society of Chemistry.* ***(F)*** *Schematic of protonation and anion adsorption in an alkaline environment. Reproduced with permission of Ref. [50] Copyright 2011, American Chemical Society.*

and determination of the amount of metal leached from the catalysts using ICP-OES found that at 25 °C, under the Ar-saturated 0.5 mol·L^{-1} H_2SO_4 condition, only a small amount of metal was leached from the two catalysts, while at 80 °C, under the O_2-saturated condition, the leached metal content was increased significantly, and the leached Fe content was lower than the Co content (Fig. 5C) (40 wt% Fe, 7.3 wt% Co), indicating that the degree of demetallation of Fe-N-C is more severe than that of Co-N-C, which significantly reduces the electrocatalyst activity [51]. The leaching of metal ions from inactive sites has little effect on the performance of the catalyst. However, when the active site is leached, the active site decreases. When the iron atom is leached in the acid medium, the strong Fenton effect makes the performance of the catalyst decline sharply.

3.2. Carbon corrosion

In M-N-C catalysts, the carbon content is as high as 85%; therefore, the corrosion of carbon makes the stability and durability of the catalyst a challenge. The oxidation of the carbon support leads to the modification of the carbon surface and, even worse, the disintegration of active sites, which can be divided into two types: electrochemical oxidation and chemical oxidation [52]. Carbon corrosion can be divided into two types: chemical and electrochemical oxidations. At voltages greater than 0.9 V, the carbon substrate becomes more susceptible to oxidation as the potential increases.

Mayrhofer and his colleagues observed carbon oxidation of Fe-NC catalysts *in situ* by using online inductively coupled plasma mass spectrometry (ICP-MS) and differential electrochemical mass spectrometry (DEMS) in combination with a modified scanning flow cell (SFC) system [19] in the oxygenated electrolyte. The CV in the electrocatalyst showed a strong oxidation current at high potentials (as shown in Fig. 5D), and the combination of ICP-MS and DEMS confirmed that the electrochemical oxidation of Fe in -NC occurred at voltages >0.9 V.

Besides the chemical and electrochemical oxidations of carbon supports, catalyst damage caused by H_2O_2/radical attack is also a significant problem hindering the development of noble metal-free catalysts. H_2O_2 may attack the catalyst in two ways: 1) direct oxidation of H_2O_2; 2) decomposition of H_2O_2 into reactive oxygen

species (ROS) through the Fenton reaction, and then ROS attacks the catalyst [53].

In 2003, Dodelet and colleagues first proposed the oxidation of ROS for electrocatalysts [51]. These reactive oxygen species, especially hydroxyl radicals (·OH), readily interact with atoms on carbon supports to form oxidized surface groups, which are detrimental to electrocatalyst activity. In addition, the highly oxidative OH not only destroys the active center of the catalyst but also easily degrades organic ionomers and membranes [54]. Jaouen and colleagues employed a rotating disk electrode (RDE) technique to explore the changes in catalyst activity and selectivity induced by hydrogen peroxide treatment [49]. The results show that the iron-based catalysts in the acidic H_2O_2-treated solution are prone to selectively oxidize the carbon atoms on the catalyst surface via the Fenton reaction without the formation of volatile CO or CO_2. This mild surface oxidation does not alter the structure of the FeN_x site but weakens the binding of the active site to O_2, thereby reducing its intrinsic activity and $4e^-$ selectivity. Afterward, some oxygen-containing functional groups on the surface were removed by electrochemical reduction or heat treatment, and it was found that the activity and selectivity could be partially recovered, indicating that the deactivation was reversible. In addition, with the increase in H_2O_2 treatment temperature, the oxygen content of the catalyst gradually increased, and the iron and nitrogen groups of the catalyst indicated did not change significantly, so it was speculated that H_2O_2 may have corroded the carbon support, resulting in an increase in the content of oxygen on the catalyst surface (Fig. 5E). Carbon corrosion may cause a loss of catalyst active site density (SD) or a decrease in active site turnover frequency (TOF), resulting in a decrease in catalyst activity [2,48,55,56].

3.3. Protonation

In general, PGM-free catalysts are more stable under alkaline conditions than under acidic conditions, and physical and electrochemical analyses suggested that the pyridine-N group is the active site of ORR, and in response to this phenomenon, Popov and colleagues proposed that the protonation reaction of pyridine-N may lead to the degradation of non-precious metal catalysts [38]. Catalysts with different N-group contents were synthesized at different pyrolysis temperatures. One catalyst containing both pyridine-N and graphite-N showed higher initial activity but lower stability; the other catalyst containing only graphitic-N showed the opposite result to the first one. The lone pair of electrons in the pyridine-N group readily binds to protons in the solution of acidic media, leading to the ORR deactivation of pyridine-N [57,58]. In contrast, graphite has no excess electrons to be protonated and it has higher stability. Later, Jaouen et al. proposed an alternative mechanism in which the surface basic N-group is protonated and then bound to the anion (Fig. 5F) [50]. The degradation of Fe-N-C catalyst activity after use can be recovered by chemical or thermal treatment, and this recovery is attributed to the removal of anions that are adsorbed on the primary nitrogen groups in an acidic environment. Thus, protonation can occur on the nitrogen group close to the FeN_x coordination structure, and then the anions adsorb onto the protonated N group by electrostatic interaction, leading to blockage and deactivation of the FeN4 active site. However, N group protonation on M-N-C catalysts is unavoidable due to the low pH environment in which PEMFCs operate [58]. Very recently, Wei and coworkers suggested that the protonation of N would weaken the Fe−N bond and ultimately result in demetallation in the form of $Fe(OH)_2$ [59]. The protonation of catalyst leads to the decrease of TOF value, resulting in the degradation of catalyst.

3.4. Microporous flooded

Based on an in-depth study of PGM-free catalysts, it was demonstrated that most of the active sites are embedded in micropores and therefore, the flooding of micropores may seriously affect the performance of the fuel cell and thus reduce the performance of the PEMFC. Dodelet et al. correlated the decay of the current density of H_2/O_2 0.6 V in the fuel cell with the micropores' flooding depending on the micropore walls' hydrophilicity [60]. The improved stability of a highly graphitic catalyst, of which the micropores were conceived to be hydrophobic and less likely to be flooded. However, Banham et al. plausibly excluded this mechanism [61]. Demetallation of FeN_4 catalytic sites in the micropores may be responsible for the rapid decay of current density in the catalyst [62].

3.5. Influence of working conditions on catalyst stability

Besides the above intrinsic mechanisms, the fuel cell's operating conditions also greatly influence the durability of the M-N-C catalysts in MEA, such as testing temperature, application potential, catalytic layer thickness, and interface impedance [63−66]. Chemical and electrochemical oxidations

occur at high temperature and high humidity; The high temperature can decrease the selectivity of the catalyst and release more H_2O_2, further accelerating the corrosion of the carbon and causing faster degradation of the catalyst. Jaouen et al. used rectangular wave cycling at high temperature and high pressure, and the results showed that the catalyst is prone to carbon corrosion at high-voltage polarization, resulting in mass transfer difficulties [43]. At the same time, the metal site of the catalyst will be lost, further resulting in the degradation of catalyst performance. Generally, the loading of catalysts used is many times that of precious metal catalysts. However, studies have shown that hydrogen peroxide formed during use can attack catalysts, resulting in a loss of activity. Jaouen et al. measured H_2O_2 yield using three $Fe_{0.5}$RP catalysts with different loads at a rotating ring disk electrode (RRDE) [67]. The study shows that the rapid increase of hydrogen peroxide production is correlated with the decrease in catalyst loading. Low catalyst loads are considered to be more genuinely representative of the selectivity of M-N-C catalysts, while high loads show lower H_2O_2 yields due to electrochemical or chemical decomposition of hydrogen peroxide, reducing the amount of peroxide detected at the ring electrode.

According to previous reports on RDE, demetallation, carbon material oxidation, and protonation will cause catalyst degradation. However, due to the significant difference between the RDE and MEA (thickness of catalysts layer, temperature, potential, and water/O_2 flux), the degradation mechanism of the MEA is much more complicated. Therefore, advanced *in-situ*/*operando* techniques are highly expected to investigate the structural evolution of M-N-C cathodes and analyze the degradation intermediates during fuel cell operation.

4. Mitigation strategies for improving stability

For transition metal catalysts, the stability and durability of electrocatalysts can be effectively improved by designing of stable active sites, enhancing the M−N bond, using of proton buffer solution, improving the corrosion resistance of carbon carriers, and reducing the Fenton effect, for the above four degradation mechanisms.

4.1. Controlling S1/S2 in Fe-N-C catalysts

Recently, Jaouen and co-workers have identified durable and nondurable Fe-N_4 sites in Fe-N-C catalysts, which may account for the two-stage decay of Fe-N-C cathode typically observed by chronoamperometry an activity−stability tradeoff in the first stage [55]. High-spin FeN_4C_{12} moiety (denoted as S1) undergoes an Fe(III)/Fe(II) redox transition (D1H/D1L) with the reversible presence of axial OH adsorbate in the region of 0−1 V, while low- or intermediate-spin FeN_4C_{10} moiety (denoted as S2) binds O_2 weakly and is potential independent (remaining D2). In operating PEMFC, S1 is nondurable and quickly transforms to ferric oxides, while S2 remains intact (Fig. 6A-B). They analyzed the results further and found that S2 sites are of both high activity and stability. Their results suggest that the seemingly identical Fe-N_x sites may have distinct fates during fuel cell operation. This study also provides new strategies for designing durable Fe-N-C catalysts under practical fuel cell: (1) increasing the site density of S2; (2) transforming S1 to more durable active sites or selectively removing S1 from the catalysts.

4.2. Strengthening M−N bonds

In non-noble metal electrocatalysts, weak M−N bonds are not conducive to atomic dispersion, thereby reducing the utilization of metal atoms and increasing the electron transfer resistance at the catalyst−support interface, thus increasing the ORR overpotential [43]. The interaction can easily lead to demetallation, which has a significant influence on the stability of the catalyst. Therefore, enhancing M−N bonds is an effective solution to improve the stability of non-noble metal catalysts. Recently, Li et al. controlled the bond length and coordination of Fe-N bonds in the catalysts by configuring different acrylic acid and maleic acid ratios to regulate the interaction between the iron ions and the polymer [68]. As shown in Fig. 6C, the Fe−N bond in the P (AA-MA) (5-1)-Fe-N catalyst has a longer bond length than that in PAA-Fe-N, and there is no significant Fe−Fe bond formation after stability tests, demonstrating the robustness of Fe-N bonds, and subsequently, the catalyst's high tolerance to Fe dementalization. Strikingly, the retention rate of performance of the P (AA-MA) (5-1)-Fe-N catalyst at the fuel cell cathode approaches 100% for the first 37 h, far better than that of PAA-Fe-N (Fig. 6D).

4.3. Buffered proton solution

At present, the relative content of protonated nitrogen species is determined by specific molecular probes and the active site density of heterogeneous electrocatalysts at different stages of the oxygen reduction reaction is determined by measuring the number of active nitrogen species

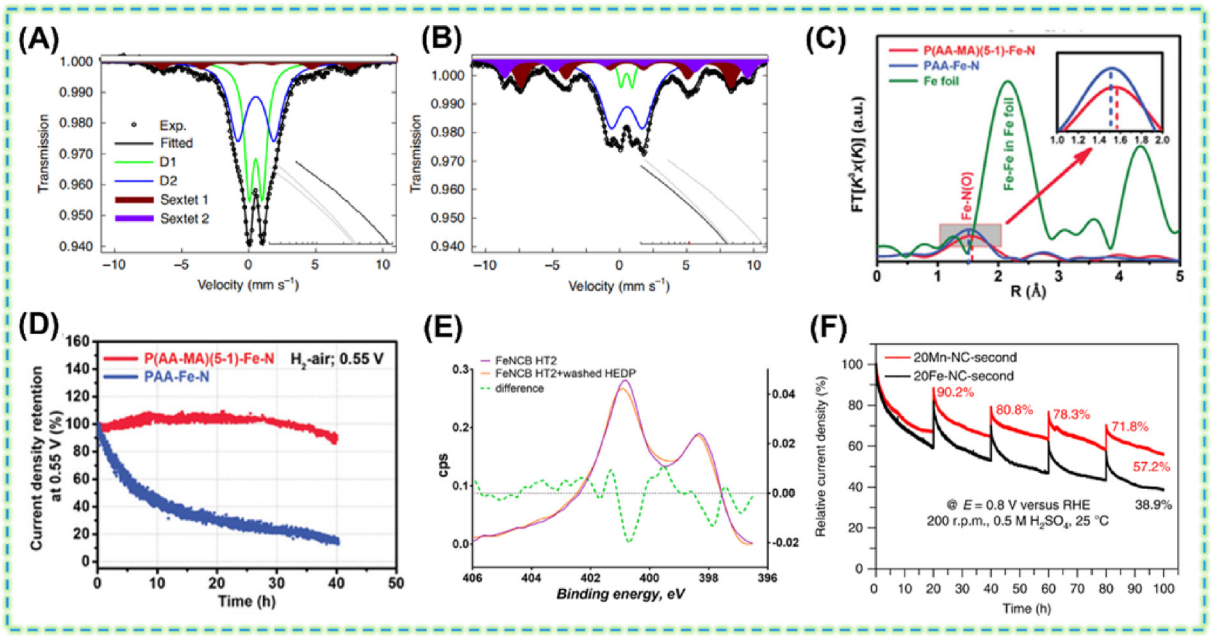

*Fig. 6. Characterization of $Fe_{0.5}$ cathode after operation at 0.5 V in PEMFC. **(A)** Ex situ ^{57}Fe Mössbauer spectrum at 5 K of the pristine $Fe_{0.5}$ cathode. Reproduced with permission of Ref. [55] Copyright 2020, Springer Nature. **(B)** EoT Mössbauer spectra at 5 K of the $Fe_{0.5}$ cathode after a hold at 0.5 V for 50 h. **(C)** k^3-weighted FT-EXAFS spectra of P (AA-MA) (5-1)-Fe-N, PAA-Fe-N, and Fe foil samples. Reproduced with permission of Ref. [68] Copyright 2021, John Wiley. **(D)** Current density retention curves of P (AA-MA) (5-1)-Fe-N and PAA-Fe-N catalysts during stability tests at a constant voltage of 0.55 V in PEMFCs. **(E)** High-resolution N 1s spectra for fresh catalyst and catalyst after exposure, and washing away HEDP overlaid spectra and difference spectra for 1000 eV·N 1s photoelectron. Reproduced with permission of Ref. [69] Copyright 2018, American Chemical Society. **(F)** i-t curves at constant potential of 0.8 V. Reproduced with permission of Ref. [7] Copyright 2018, Springer Nature.*

[57,69]. By using a nitrogen-free active molecular probe (bisphosphonate chelator 1-hydroxyethane 1,1-diphosphonic acid, HEDP), Artyushkova et al. found that HEDP was associated with protonated nitrogen species closely, binding different nitrogen species on the catalyst surface. The nitrogen species concentration distribution at different sampling depths was demonstrated by high-resolution N 1s spectroscopy (Fig. 6E for 2 nm on the surface). Comparing the presence and absence of HEDP adsorption catalyst, it was found that HEDP mainly blocked the protonated nitrogen atoms. The complexing agent/buffer impedes the protonation of the active N site, thus reducing the occurrence of partial reduction of oxygen to H_2O_2, which is beneficial for improving the stability of the catalyst.

4.4. Improving carbon corrosion resistance

Improving the corrosion resistance of carbon can enhance the degree of graphitization of carbon supports by controlling the ligand structure and thermal activation conditions. Surface fluorination of carbon can change the coordination structure of carbon, which is beneficial to enhancing oxidative stability [70,71]. In addition, the incorporation of metal elements can also improve the corrosion resistance of carbon [53]. For example, Wu et al. prepared FeCoNiMn-NC electrocatalysts for oxygen reduction by a template-free carbonization method [72]. Due to the incorporation of Mn, the degree of graphitization of the thick and dense carbon support was improved, and at the same time, it was favorable for the formation of active metal oxides. For the control of thermal activation conditions, Wu et al. group prepared a hierarchical porous carbon nanofiber network with a high degree of graphitization by electrospinning [42]. The first step of this step-by-step pyrolysis strategy is to generate porosity at a lower temperature, and followed by generating atomically dispersed active CoN_4 sites at the higher temperature.

4.5. Exploring the low Fenton reactivity catalysts

Iron ions have been criticized for their catalytic effect on the decomposition of H_2O_2 to ROS. However, Fe-free transition metals, such as Cr, Mn, Co, Ni, Cu, and Zn are not powerful Fenton reagents. Therefore, M-N-C catalysts based on these iron-free metals have the potential to mitigate the Fenton reaction. Wu et al. prepared a Mn-N-C catalyst with lower Fenton reactivity, which was determined by electrochemical analysis to be

close to the ORR reactivity of Fe-N-C catalyst, and its stability in acidic media was significantly enhanced [7]. Fig. 6F is the durability test graph of Mn-N-C and Fe-N-C, showing the more serious irreversible degradation of Fe-N-C. After that, his research group used strong ligand exchange to prepare atomically dispersed cobalt and nitrogen co-doped carbon electrocatalysts, which have activity comparable to Fe-N-C and have much higher durability than Fe [36]. Ge et al. prepared a Cr-N-C single-atom catalyst with superior stability for the first time, and used Cr-N-C to analyze the effects of H_2O_2 and ROS on the catalyst performance through the Fenton reaction [73]. ABTS was used as a molecular probe to assess the production level of reactive oxygen species. ABTS can be oxidized by ROS, and the visual color can be changed from colorless to green. The oxidation of ABTS can be shown from the UV/Vis absorption spectrum at 417 nm, and the absorbance value of Cr-NC is only 4.3% of that of Fe-NC counterpart, thus clearly demonstrating that Cr-NC acts as a catalyst to inhibit ROS. Formed, that is, inhibited the occurrence of the Fenton reaction.

In addition to 3d transition metal-N_x moieties, M-N-C catalysts based on s- and p-block elements were also discovered with ORR activities in acid media [74−76]. Strasser and co-workers reported Sn-N-C catalysts with the TOF comparable to state-of-the-art Fe-N-C [74]. Their results revealed that the Sn-N_x active sites break the commonly accepted scaling relationships and maintain a constant oxygen chemisorption energy that favored the $4e^-$ ORR process. Similarly, Jiao and co-workers demonstrated that the main-group metals in s-block could possess excellent ORR activity in acid media if coordinated with N or N/O, which moved the p-orbital center close to the Fermi level [75]. All in all, selecting transition metals or main group elements with lower Fenton reactivity to prepare electrocatalysts is the most effective way to reduce the Fenton effect [77−80].

5. Summary and prospects

In this review, we summarize the recent development of PGM-free cathode catalysts, primarily based on our effort in the past years. Significant progress has been achieved in improving catalyst activity/stability and promising MEA performance, bringing the PGM-free catalyst technology closer to possible viable applications in the future. In particular, the state-of-the-art PGM-free catalyst can demonstrate initial fuel cell performance similar to that of a commercial Pt/C. However, the loading of a PGM-free catalyst is much higher than that of PGM catalysts. Several promising strategies to further enhance the activity include but are not limited to, spatial confinement, chemical confinement, spin state regulation, or tuning the mesopore structure. The ultimate commercial viability of these strategies would require catalyst synthesis routes that are scalable.

Despite the promising activity, a remaining barrier to the commercialization of PGM-free fuel cell catalysts is the instability of the catalyst or the electrodes in the fuel cell system. These active sites may be severely damaged by acid and hydroxyl group to MN_4 active center and may also be affected by hydrogen peroxide and anionic adsorption, resulting in the reduction of MN_4 intrinsic activity, as well as possible ionomer phase changes and flooding in the cathode, which will also lead to additional material transport resistance, and proton/electron transfer resistance. The internal stability of M-N-C catalyst can be improved via the following strategies: (i) designing of stable active sites; (ii) designing local coordination structure to strengthen M−N bond; (iii) buffer is introduced to reduce the influence of protonation on the catalyst; (iv) increased graphitization with stronger carbon carriers to mitigate carbon oxidation; (v) using Fe-free catalyst to weaken Fenton's effect thus to reduce the production of hydroxyl intermediates;

Although promising achievements have been made in understanding the activity and degradation mechanisms, one major remaining barrier to the commercialization of M-N-C fuel cell catalysts is the instability of the M-N-C catalyst or the electrodes in the practical fuel cell system. The widespread mechanisms can partly answer why Fe-N-C degrades in operating fuel cells. More important questions that have to be addressed are what kinds of active sites are intrinsically stable and how to prepare such sites selectively. The following efforts may speed up this process:

(i) Advanced *in situ*/*operando* techniques are highly expected to investigate the structural evolution of M-N-C cathodes and analyze the degradation intermediates during fuel cell operation. Generally, the subtle structural variations of FeN_xC_y moieties often lead to a notable difference in stability. Such advanced techniques can further provide the relationship between specific structural parameters/descriptors and stability.

(ii) Significant research efforts toward advanced stability prediction methods will be crucial in the future. The theoretical simulations should consider the complex degradation process, especially coupled degradation mechanisms and the influence of the external environmental fields should be considered.

(iii) Exploring carbon-free support. Carbon corrosion is thermodynamically inevitable during the operation of fuel cells, especially the uncontrollable high potential occurred in the starts/stops. Accordingly, it might be the ultimate solution to explore corrosion-resistant carbon-free support.

(iv) Developing new ionomers with electrochemical stability is essential to achieving highly active and stable MEA. Metal leaching of catalysts can reduce the catalyst conductivity and cause catalyst degradation. The development of new ion exchange membranes with good stability can attenuate the catalyst impact on fuel cell performance.

Overall, the development of atomically dispersed M-N-C catalysts to replace PGM catalysts is highly rewarding for fuel cell technology. The extensive research should focus on addressing serious stability issues and improving the performance of MEA in the future.

Acknowledgements

This work was financially supported by the National Natural Science Foundation of China (No. 21875221 and No. 22102156), Distinguished Young Scholars Innovation Team of Zhengzhou University (No. 32320275), Academic Degrees & Graduate Education Reform Project of Henan Province (2021 SJGLX 093Y) and China Postdoctoral Science Foundation (2021TQ0295).

References

[1] Banham D, Ye S, Pei K, Ozaki J, Kishimoto T, Imashiro Y. A review of the stability and durability of non-precious metal catalysts for the oxygen reduction reaction in proton exchange membrane fuel cells[J]. J. Power Sources, 2015, 285: 334−348.

[2] Wan X, Liu X F, Shui J L. Stability of PGM-free fuel cell catalysts: degradation mechanisms and mitigation strategies[J]. Prog. Nat. Sci., 2020, 30(6): 721−731.

[3] Chen Z Y, Niu H, Ding J, Liu H, Chen P H, Lu Y H, Lu Y R, Zuo W B, Han L, Guo Y Z, Hung S F, Zhai Y M. Unraveling the origin of sulfur-doped Fe-N-C single-atom catalyst for enhanced oxygen reduction activity: effect of iron spin-state tuning[J]. Angew. Chem. Int. Ed., 2021, 60(48): 25404−25410.

[4] Jiao L, Li J K, Richard L L, Sun Q, Stracensky T, Liu E R, Sougrati M T, Zhao Z P, Yang F, Zhong S C, Xu H, Mukerjee S, Huang Y, Cullen D A, Park J H, Ferrandon M, Myers D J, Jaouen F, Jia Q Y. Chemical vapour deposition of Fe-N-C oxygen reduction catalysts with full utilization of dense Fe-N_4 sites[J]. Nat. Mater., 2021, 20(10): 1385−1391.

[5] Wan X, Liu X F, Li Y C, Yu R H, Zheng L R, Yan W S, Wang H, Xu M, Shui J L. Fe-N-C electrocatalyst with dense active sites and efficient mass transport for high-perfor-mance proton exchange membrane fuel cells[J]. Nat. Catal., 2019, 2(3): 259−268.

[6] Mehmood A, Gong M J, Jaouen F, Roy A, Zitolo A, Khan A, Sougrati M T, Primbs M, Bonastres A M, Fongalland D, Drazic G, Strasser P, Kucernak A. High loading of single atomic iron sites in Fe-NC oxygen reduction catalysts for proton exchange membrane fuel cells[J]. Nat. Catal., 2022, 5(4): 311−323.

[7] Li J Z, Chen M J, Cullen D A, Hwang S, Wang M Y, Li B Y, Liu K X, Karakalos S, Lucero M, Zhang H G, Lei C, Xu H, Sterbinsky G E, Feng Z X, Su D, More K L, Wang G F, Wang Z B, Wu G. Atomically dispersed manganese catalysts for oxygen reduction in proton-exchange membrane fuel cells[J]. Nat. Catal., 2018, 1(12): 935−945.

[8] Zhang H G, Chung H T, Cullen D A, Wagner S, Kramm U I, More K L, Zelenay P, Wu G. High-performance fuel cell cathodes exclusively containing atomically dispersed iron active sites[J]. Energy Environ. Sci., 2019, 12(8): 2548−2558.

[9] He Y H, Hwang S, Cullen D A, Uddin M A, Langhorst L, Li B Y, Karakalos S, Kropf A J, Wegener E C, Sokolowski J, Chen M J, Myers D, Su D, More K L, Wang G F, Litster S, Wu G. Highly active atomically dispersed CoN_4 fuel cell cathode catalysts derived from surfactant-assisted MOFs: carbon-shell confinement strategy[J]. Energy Environ. Sci., 2019, 12(1): 250−260.

[10] Yin H B, Xia H C, Zhao S Y, Li K X, Zhang J N, Mu S C. Atomic level dispersed metal-nitrogen-carbon catalyst toward oxygen reduction reaction: synthesis strategies and chemical environmental regulation[J]. Energy Environ. Mater., 2021, 4(1): 5−18.

[11] Zhao S Y, Yin H B, Xia H C, Qu G, Yi S S, Pang H, Yan W F, Zhang J N, Mu S C. The assembling principle and strategies of high-density atomically dispersed catalysts[J]. Chem. Eng. J. 2021: 417.

[12] Guo S Y, Yuan P F, Zhang J A, Jin P B, Sun H M, Lei K X, Pang X C, Xu Q, Cheng F Y. Atomic-scaled cobalt encapsulated in P,N-doped carbon sheaths over carbon nanotubes for enhanced oxygen reduction electrocatalysis under acidic and alkaline media[J]. Chem. Commun., 2017, 53(71): 9862−9865.

[13] Zhao S N, Li J K, Wang R, Cai J M, Zang S Q. Electronically and geometrically modified single-atom Fe sites by adjacent Fe nanoparticles for enhanced oxygen reduction[J]. Adv. Mater., 2022, 34(5): e2107291.

[14] Schulenburg H, Stankov S, Schunemann V, Radnik J, Dorbandt I, Fiechter S, Bogdanoff P, Tributsch H. Catalysts for the oxygen reduction from heat-treated iron(III) tetramethoxyphenylporphyrin chloride: structure and stability of active sites[J]. J. Phys. Chem. B, 2003, 107(34): 9034−9041.

[15] Litster S, Wu G, Xu H. 2021 US DOE Hydrogen and Fuel Cell Technologies Annual Meeting: Advanced PGM-free Cathode Engineering for High Power Density and durability, 2021[C]. Pittsburgh: Carnegie Mellon University, 2021.

[17] Chen G B, An Y, Liu S W, Sun F F, Qi H Y, Wu H F, He Y H, Liu P, Shi R, Zhang J, Kuc A, Kaiser U, Zhang T R, Heine T, Wu G, Feng X L. Highly accessible and dense surface single metal FeN_4 active sites for promoting the oxygen reduction reaction[J]. Energy Environ. Sci., 2022, 15(6): 2619−2628.

[18] Guo J N, Li B J, Zhang Q Y, Liu Q T, Wang Z L, Zhao Y F, Shui J L, Xiang Z H. Highly accessible atomically dispersed Fe-Nx sites electrocatalyst for proton-exchange membrane fuel cell[J]. Adv. Sci., 2021, 8(5): 2002249.

[19] Choi C H, Baldizzone C, Grote J P, Schuppert A K, Jaouen F, Mayrhofer K JJ. Stability of Fe-N-C catalysts in acidic medium studied by operando spectroscopy[J]. Angew. Chem. Int. Ed., 2015, 54(43): 12753−12757.

[20] Du L, Prabhakaran V, Xie X H, Park S, Wang Y, Shao Y Y. Low-PGM and PGM-free catalysts for proton exchange

membrane fuel cells: stability challenges and material solutions[J]. Adv. Mater., 2021, 33(6): e1908232.
[21] Cheng W Z, Yuan P F, Lv Z R, Guo Y Y, Qiao Y Y, Xue X Y, Liu X, Bai W L, Wang K X, Xu Q, Zhang J N. Boosting defective carbon by anchoring well-defined atomically dispersed metal-N_4 sites for ORR, OER, and Zn-air batteries[J]. Appl. Catal. B 2020: 260.
[22] Cheng W Z, Liang J L, Yin H B, Wang Y J, Yan W F, Zhang J N. Bifunctional iron-phtalocyanine metal-organic framework catalyst for ORR, OER and rechargeable zinc-air battery[J]. Rare Met., 2020, 39(7): 815−823.
[23] Guo Y Y, Yuan P F, Zhang J N, Hu Y F, Amiinu I S, Wang X, Zhou J G, Xia H C, Song Z B, Xu Q, Mu S C. Carbon nanosheets containing discrete Co-Nx-By-C active sites for efficient oxygen electrocatalysis and rechargeable Zn-air batteries[J]. ACS Nano, 2018, 12(2): 1894−1901.
[24] Guo Y Y, Yuan P F, Zhang J A, Xia H C, Cheng F Y, Zhou M F, Li J, Qiao Y Y, Mu S C, Xu Q. Co_2P-CoN double active centers confined in N-doped carbon nanotube: heterostructural engineering for trifunctional catalysis toward HER, ORR, OER, and Zn-air batteries driven water splitting [J]. Adv. Funct. Mater., 2018, 28(51): 1805641.
[25] Qiao Y Y, Yuan P F, Hu Y F, Zhang J N, Mu S C, Zhou J H, Li H, Xia H C, He J, Xu Q. Sulfuration of an Fe-N-C catalyst containing Fe_xC/Fe species to enhance the catalysis of oxygen reduction in acidic media and for use in flexible Zn-air batteries[J]. Adv. Mater., 2018, 30(46): e1804504.
[26] Wang M, Zhang C T, Meng T, Pu Z H, Jin H H, He D P, Zhang J N, Mu S C. Iron oxide and phosphide encapsulated within N,P-doped microporous carbon nanofibers as advanced tri-functional electrocatalyst toward oxygen reduction/evolution and hydrogen evolution reactions and zinc-air batteries[J]. J. Power Sources, 2019, 413: 367−375.
[27] Xue X Y, Yang H, Yang T, Yuan P F, Li Q, Mu S C, Zheng X L, Chi L F, Zhu J, Li Y G, Zhang J N, Xu Q N. P-coordinated fullerene-like carbon nanostructures with dual active centers toward highly-efficient multi-functional electrocatalysis for CO_2RR, ORR and Zn-air battery[J]. J. Mater. Chem., 2019, 7(25): 15271−15277.
[28] Yang G G, Zhu J W, Yuan P F, Hu Y F, Qu G, Lu B A, Xue X Y, Yin H B, Cheng W Z, Cheng J Q, Xu W J, Li J, Hu J S, Mu S C, Zhang J N. Regulating Fe-spin state by atomically dispersed Mn-N in Fe-N-C catalysts with high oxygen reduction activity [J]. Nat. Commun., 2021, 12(1): 1734.
[29] Yin H B, Yuan P F, Lu B A, Xia H C, Guo K, Yang G G, Qu G, Xue D P, Hu Y F, Cheng J Q, Mu S C, Zhang J N. Phosphorus-driven electron delocalization on edge-type FeN_4 active sites for oxygen reduction in acid medium[J]. ACS Catal., 2021, 11(20): 12754−12762.
[30] Zhu J W, Li W Q, Li S H, Zhang J, Zhou H, Zhang C T, Zhang J A, Mu S C. Defective N/S-codoped 3D cheese-like porous carbon nanomaterial toward efficient oxygen reduction and Zn-air batteries[J]. Small, 2018, 14(21): e1800563.
[31] Qu X M, Han Y, Chen Y H, Lin J X, Li G, Yang J, Jiang Y X, Sun S G. Stepwise pyrolysis treatment as an efficient strategy to enhance the stability performance of Fe-N_x/C electrocatalyst towards oxygen reduction reaction and proton exchange membrane fuel cell[J]. Appl. Catal. B Environ., 2021, 295: 120311.
[32] Wang X X, Cullen D A, Pan Y T, Hwang S, Wang M Y, Feng Z X, Wang J Y, Engelhard M H, Zhang H G, He Y H, Shao Y Y, Su D, More K L, Spendelow J S, Wu G. Nitrogen-coordinated single cobalt atom catalysts for oxygen reduction in proton exchange membrane fuel cells[J]. Adv. Mater., 2018, 30(11): 1706758.
[33] Lai Q X, Zheng L R, Liang Y Y, He J P, Zhao J X, Chen J H. Metal-organic-framework-derived Fe-N/C electrocatalyst with five-coordinated Fe-N_x sites for advanced oxygen reduction in acid media[J]. ACS Catal., 2017, 7(3): 1655−1663.
[34] Yu L, Deng D H, Bao X H. Chain mail for catalysts[J]. Angew. Chem. Int. Ed., 2020, 59(36): 15294−15297.
[35] Yang G G, Zhu J W, Yuan P F, Hu Y F, Qu G, Lu B A, Xue X Y, Yin H B, Cheng W Z, Cheng J Q, Xu W J, Li J, Hu J S, Mu S C, Zhang J N. Regulating Fe-spin state by atomically dispersed Mn-N in Fe-N-C catalysts with high oxygen reduction activity[J]. Nat. Commun., 2021, 12(1): 1734.
[36] Xie X H, He C, Li B Y, He Y H, Cullen D A, Wegener E C, Kropf A J, Martinez U, Cheng Y W, Engelhard M H, Bowden M E, Song M, Lemmon T, Li X S, Nie Z M, Liu J, Myers D J, Zelenay P, Wang G F, Wu G, Ramani V, Shao Y Y. Performance enhancement and degradation mechanism identification of a single-atom Co-N-C catalyst for proton exchange membrane fuel cells[J]. Nat. Catal., 2020, 3(12): 1044−1054.
[37] Liu G, Li X G, Popov B N. Stability study of nitrogen-modified carbon composite catalysts for oxygen reduction reaction in polymer electrolyte membrane fuel cells[J]. ECS Trans., 2009, 25(1): 1251−1259.
[38] Liu G, Li X G, Ganesan P, Popov B N. Studies of oxygen reduction reaction active sites and stability of nitrogen-modified carbon composite catalysts for PEM fuel cells[J]. Electrochim. Acta, 2010, 55(8): 2853−2858.
[39] Chenitz R, Kramm U I, Lefevre M, Glibin V, Zhang G X, Sun S H, Dodelet J P. A specific demetalation of Fe-N_4 catalytic sites in the micropores of NC-Ar + NH_3 is at the origin of the initial activity loss of the highly active Fe/N/C catalyst used for the reduction of oxygen in PEM fuel cells [J]. Energy Environ. Sci., 2018, 11(2): 365−382.
[40] Prabhakaran V, Wang G X, Parrondo J, Ramani V. Contribution of electrocatalyst support to PEM oxidative degradation in an operating PEFC[J]. J. Electrochem. Soc., 2016, 163(14): F1611−F1617.
[41] Zhao L, Zhu J B, Zheng Y, Xiao M L, Gao R, Zhang Z, Wen G B, Dou H Z, Deng Y P, Yu A P, Wang Z B, Chen Z W. Materials engineering toward durable electrocatalysts for proton exchange membrane fuel cells[J]. Adv. Energy Mater., 2021, 12(2): 2102665.
[42] Wang X L, Yang C, Wang X G, Zhu H W, Cao L J, Chen A Y, Gu L, Zhang Q H, Zheng L R, Liang H P. Green synthesis of a highly efficient and stable single-atom iron catalyst anchored on nitrogen-doped carbon nanorods for the oxygen reduction reaction[J]. ACS Sustainable Chem. Eng., 2020, 9(1): 137−146.
[43] Goellner V, Baldizzone C, Schuppert A, Sougrati M T, Mayrhofer K, Jaouen F. Degradation of Fe/N/C catalysts upon high polarization in acid medium[J]. Phys. Chem. Chem. Phys., 2014, 16(34): 18454−18462.
[44] Choi C H, Baldizzone C, Polymeros G, Pizzutilo E, Kasian O, Schuppert A K, Sahraie N R, Sougrati M T, Mayrhofer K JJ, Jaouen F. Minimizing operando demetallation of Fe-N-C electrocatalysts in acidic medium[J]. ACS Catal., 2016, 6(5): 3136−3146.
[45] Chen Z, Jiang S, Kang G, Nguyen D, Schatz G C, Van duyne R P. Operando characterization of iron phthalocyanine deactivation during oxygen reduction reaction using electrochemical tip-enhanced Raman spectroscopy[J]. J. Am. Chem. Soc., 2019, 141(39): 15684−15692.
[46] Snitkoff-sol R Z, Friedman A, Honig H C, Yurko Y, Kozhushner A, Zachman M J, Zelenay P, Bond A M, Elbaz L. Quantifying the electrochemical active site density of precious metal-free catalysts *in situ* in fuel cells[J]. Nat. Catal., 2022, 5(2): 163−170.
[47] Wei X, Wang R Z, Zhao W, Chen G, Chai M R, Zhang L, Zhang J J. Recent research progress in PEM fuel cell

electrocatalyst degradation and mitigation strategies[J]. EnergyChem, 2021, 3(5).

[48] He Y H, Wu G. PGM-Free oxygen-reduction catalyst development for proton-exchange membrane fuel cells: challenges, solutions, and promises[J]. Accounts Mater. Res., 2022, 3(2): 224−236.

[49] Choi C H, Lim H K, Chung M W, Chon G, Sahraie N R, Altin A, Sougrati M T, Stievano L, Oh H S, Park E S, Luo F, Strasser P, Drazic G, Mayrhofer K JJ, Kim H, Jaouen F. The Achilles' heel of iron-based catalysts during oxygen reduction in an acidic medium[J]. Energy Environ. Sci., 2018, 11(11): 3176−3182.

[50] Herranz J, Jaouen F, Lefevre M, Kramm U I, Proietti E, Dodelet J P, Bogdanoff P, Fiechter S, Abs-wurmbach I, Bertrand P, Arruda T M, Mukerjee S. Unveiling N-protonation and anion-binding effects on Fe/N/C-catalysts for O_2 reduction in PEM fuel cells[J]. J. Phys. Chem. C, 2011, 115(32): 16087−16097.

[51] Lefevre M, Dodelet J P. Fe-based catalysts for the reduction of oxygen in polymer electrolyte membrane fuel cell conditions: determination of the amount of peroxide released during electroreduction and its influence on the stability of the catalysts[J]. Electrochim. Acta, 2003, 48(19): 2749−2760.

[52] Preger Y, Gerken J B, Biswas S, Anson C W, Johnson M R, Root T W, Stahl S S. Quinone-mediated electrochemical O_2 reduction accessing high power density with an off-electrode Co-N/C catalyst[J]. Joule, 2018, 2(12): 2722−2731.

[53] Zhang P Y, Wang Y C, You Y Z, Yuan J Y, Zhou Z Y, Sun S G. Generation pathway of hydroxyl radical in Fe/N/C-based oxygen reduction electrocatalysts under acidic media[J]. J. Phys. Chem. Lett., 2021, 12(32): 7797−7803.

[54] Gubler L, Dockheer S M, Koppenol W H. Radical ($HO^{\bullet}$, $H^{\bullet}$ and $HOO^{\bullet}$) formation and ionomer degradation in polymer electrolyte fuel cells[J]. J. Electrochem. Soc., 2011, 158(7): B755−B769.

[55] Li J K, Sougrati M T, Zitolo A, Ablett J M, Oguz I C, Mineva T, Matanovic I, Atanassov P, Huang Y, Zenyuk I, Di cicco A, Kumar K, Dubau L, Maillard F, Drazic G, Jaouen F. Identification of durable and non-durable FeN_x sites in Fe-N-C materials for proton exchange membrane fuel cells[J]. Nat. Catal., 2020, 4(1): 10−19.

[56] Wang X X, Swihart M T, Wu G. Achievements, challenges and perspectives on cathode catalysts in proton exchange membrane fuel cells for transportation[J]. Nat. Catal., 2019, 2(7): 578−589.

[57] Mamtani K, Jain D, Zemlyanov D, Celik G, Luthman J, Renkes G, Co A C, Ozkan U S. Probing the oxygen reduction reaction active sites over nitrogen-doped carbon nanostructures (CN_x) in acidic media using phosphate anion[J]. ACS Catal., 2016, 6(10): 7249−7259.

[58] Rauf M, Zhao Y D, Wang Y C, Zheng Y P, Chen C, Yang X D, Zhou Z Y, Sun S G. Insight into the different ORR catalytic activity of Fe/N/C between acidic and alkaline media: protonation of pyridinic nitrogen[J]. Electrochem. Commun., 2016, 73: 71−74.

[59] Yang N, Peng L L, Li L, Li J, Liao Q, Shao M H, Wei Z D. Theoretically probing the possible degradation mechanisms of an FeNC catalyst during the oxygen reduction reaction[J]. Chem. Sci., 2021, 12(37): 12476−12484.

[60] Zhang G X, Chenitz R, Lefevre M, Sun S H, Dodelet J P. Is iron involved in the lack of stability of Fe/N/C electrocatalysts used to reduce oxygen at the cathode of PEM fuel cells?[J]. Nano Energy, 2016, 29: 111−125.

[61] Choi J Y, Yang L J, Kishimoto T, Fu X G, Ye S Y, Chen Z W, Banham D. Is the rapid initial performance loss of Fe/N/C non precious metal catalysts due to micropore flooding?[J]. Energy Environ. Sci., 2017, 10(1): 296−305.

[62] Chenitz R, Kramm U I, Lefevre M, Glibin V, Zhang G X, Sun S H, Dodelet J P. A specific demetalation of $Fe-N_4$ catalytic sites in the micropores of NC-Ar + NH_3 is at the origin of the initial activity loss of the highly active Fe/N/C catalyst used for the reduction of oxygen in PEM fuel cells [J]. Energy Environ. Sci., 2018, 11(2): 365−382.

[63] Mustain W E, Chatenet M, Page M, Kim Y S. Durability challenges of anion exchange membrane fuel cells[J]. Energy Environ. Sci., 2020, 13(9): 2805−2838.

[64] Deng D H, Yu L, Chen X Q, Wang G X, Jin L, Pan X L, Deng J, Sun G Q, Bao X H. Iron encapsulated within pod-like carbon nanotubes for oxygen reduction reaction[J]. Angew. Chem. Int. Ed., 2013, 52(1): 371−375.

[65] Bhosale A C, Rengaswamy R. Interfacial contact resistance in polymer electrolyte membrane fuel cells: recent developments and challenges[J]. Renew. Sustain. Energy Rev., 2019, 115.

[66] Banham D, Kishimoto T, Sato T, Kobayashi Y, Narizuka K, Ozaki J I, Zhou Y, Marquez E, Bai K, Ye S. New insights into non-precious metal catalyst layer designs for proton exchange membrane fuel cells: improving performance and stability[J]. J. Power Sources, 2017, 344: 39−45.

[67] Kumar K, Dubau L, Mermoux M, Li J K, Zitolo A, Nelayah J, Jaouen F, Maillard F. On the influence of oxygen on the degradation of Fe-N-C catalysts[J]. Angew. Chem. Int. Ed., 2020, 59(8): 3235−3243.

[68] Miao Z P, Wang X M, Zhao Z L, Zuo W B, Chen S Q, Li Z Q, He Y H, Liang J S, Ma F, Wang H L, Lu G, Huang Y H, Wu G, Li Q. Improving the stability of non-noble-metal M-N-C catalysts for proton-exchange-membrane fuel cells through M-N bond length and coordination regulation[J]. Adv. Mater., 2021, 33(39): e2006613.

[69] Chen Y C, Matanovic I, Weiler E, Atanassov P, Artyushkova K. Mechanism of oxygen reduction reaction on transition metal-nitrogen-carbon catalysts: establishing the role of nitrogen-containing active sites[J]. ACS Appl. Energy Mater., 2018, 1(11): 5948−5953.

[70] Zhang G X, Yang X H, Dubois M, Herraiz M, Chenitz R, Lefevre M, Cherif M, Vidal F, Glibin V P, Sun S H, Dodelet J P. Non-PGM electrocatalysts for PEM fuel cells: effect of fluorination on the activity and stability of a highly active NC-Ar + NH_3 catalyst[J]. Energy Environ. Sci., 2019, 12(10): 3015−3037.

[71] Chang J F, Wang G Z, Wang M Y, Wang Q, Li B Y, Zhou H, Zhu Y M, Zhang W, Omer M, Orlovskaya N, Ma Q, Gu M, Feng Z X, Wang G F, Yang Y. Improving Pd-N-C fuel cell electrocatalysts through fluorination-driven rearrangements of local coordination environment[J]. Nat. Energy, 2021, 6(12): 1144−1153.

[72] Gupta S, Zhao S, Wang X X, Hwang S, Karakalos S, Devaguptapu S V, Mukherjee S, Su D, Xu H, Wu G. Quaternary FeCoNiMn-based nanocarbon electrocatalysts for bifunctional oxygen reduction and evolution: promotional role of Mn doping in stabilizing carbon[J]. ACS Catal., 2017, 7(12): 8386−8393.

[73] Luo E G, Zhang H, Wang X, Gao L Q, Gong L Y, Zhao T, Jin Z, Ge J J, Jiang Z, Liu C P, Xing W. Single-atom Cr-N_4 sites designed for durable oxygen reduction catalysis in acid media[J]. Angew. Chem. Int. Ed., 2019, 58(36): 12469−12475.

[74] Luo F, Roy A R, Silvioli L, Cullen D A, Zitolo A, Sougrati M T, Oguz I C, Mineva T, Teschner D, Wagner S, Wen J, Dionigi F, Kramm U I, Rossmeisl J, Jaouen F, Strasser P. P-block single-metal-site tin/nitrogen-doped carbon fuel cell cathode catalyst for oxygen reduction reaction[J]. Nat. Mater., 2020, 19(11): 1215−1223.

[75] Wang T Z, Cao X J, Qin H Y, Shang L, Zheng S Y, Fang F, Jiao L F. P-block atomically dispersed antimony catalyst for

highly efficient oxygen reduction reaction[J]. Angew. Chem. Int. Ed., 2021, 60(39): 21237−21241.
[76] Hu H, Wang J J, Cui B F, Zheng X R, Lin J G, Deng Y D, Han X P. Atomically dispersed selenium sites on nitrogen-doped carbon for efficient electrocatalytic oxygen reduction [J]. Angew. Chem. Int. Ed., 2022, 61(3): e202114441.
[77] Zhu J W, Mu S C. Active site engineering of atomically dispersed transition metal-heteroatom-carbon catalysts for oxygen reduction[J]. Chem. Commun., 2021, 57(64): 7869−7881.
[78] Jin H H, Zhu J W, Yu R H, Li W Q, Ji P X, Liang L H, Liu B S, Hu C X, He D P, Mu S C. Tuning the Fe−N_4 sites by introducing Bi−O bonds in a Fe-N-C system for promoting the oxygen reduction reaction[J]. J. Mater. Chem., 2022, 10(2): 664−671.
[79] Ma L G, Li J L, Zhang Z W, Yang H, Mu X Q, Gu X Y, Jin H H, Chen D, Yan S L, Liu S L, Mu S C. Atomically dispersed dual Fe centers on nitrogen-doped bamboo-like carbon nanotubes for efficient oxygen reduction[J]. Nano Res., 2021, 15(3): 1966−1972.
[80] Zhang J, Zhang J J, He F, Chen Y J, Zhu J W, Wang D L, Mu S C, Yang H Y. Defect and doping Co-engineered non-metal nanocarbon ORR electrocatalyst[J]. Nano-Micro Lett., 2021, 13(1): 65.

高活性和耐久性非铂氧还原催化剂的研究进展

李　渊，陈妙迎，卢帮安*，张佳楠*
郑州大学材料科学与工程学院，河南 郑州 450001

摘要

质子交换膜燃料电池（PEMFCs）阴极氧还原反应（ORR）动力学迟缓，需要消耗大量的贵金属催化剂，这限制了其商业化应用。目前，原子级分散的 M-N-C（M = Fe, Co, Mn 等）催化剂受到人们青睐，有望替代铂催化剂。在过去的几十年里，M-N-C 催化剂取得了很大的进步，具有优异的 ORR 活性，而且燃料电池初始性能有希望接近传统的 Pt/C 催化剂。然而，这些高活性的 Fe-N-C 催化剂在燃料电池实际工作条件下的稳定性比较差。这篇综述总结了在高效氧还原 M-N-C 催化剂方面的最近进展，主要概述了作者课题组在限域策略和自旋调控方面的贡献。此外，我们还总结了几种提高活性的有效方法以及近期的关于揭示 M-N-C 催化剂的降解机制的认识，如金属浸出、碳腐蚀、质子化和微孔淹没都会造成催化剂降解。为改善 M-N-C 催化剂的寿命，我们概括了文献中的缓解策略，包括控制催化剂中 S1/S2 位点、使用非铁基催化剂、增强金属氮键、改善碳载体的耐腐蚀性和使用质子缓冲液等。最后，提出了目前原子级分散的 M-N-C 催化剂的存在的挑战和可能的解决方案。

关键字：非贵金属催化剂；限域策略；自旋调控；降解机理；缓解策略